# An effective method for separating casting components from the runner system using vibration-induced fatigue damage

**Article** *in* The International Journal of Advanced Manufacturing Technology · October 2014

DOI: 10.1007/s00170-014-6077-z

CITATIONS
16

READS
1,015

**3 authors**, including:

Pei-Hsing Huang
National Yunlin University of Science and Technology
**69** PUBLICATIONS **573** CITATIONS

SEE PROFILE

Bor-Tsuen Wang
National Pingtung University of Science and Technology
**59** PUBLICATIONS **1,105** CITATIONS

SEE PROFILE

Int J Adv Manuf Technol (2014) 74:1275–1282
DOI 10.1007/s00170-014-6077-z

ORIGINAL ARTICLE

# An effective method for separating casting components from the runner system using vibration-induced fatigue damage

**Pei-Hsing Huang · Yu-Ting Chen · Bor-Tsuen Wang**

Received: 11 December 2013 / Accepted: 16 June 2014 / Published online: 27 June 2014


**Abstract** In the final step of the investment casting process, the casting components have to be cutoff at the ingate from the main sprue or the runner system. Cutting the ingates is normally performed using a grinding wheel cutting machine, which is dangerous and consumes a great deal of labor and time. This work thus introduces a vibration method for separating casting parts from the casting tree. First, a V-shaped notch near the ingate of the runner is designed in order to generate the stress concentration effect during the induced vibration process by a pneumatic hammer. Then, the structural modal properties of the casting tree are analyzed to derive the natural frequencies and mode shapes. The flexible modal vibration of the casting parts due to resonance effect during excited vibration will cause fatigue damage at the notch, allowing the castings to be removed from the tree. Mold flow analyses are conducted to design the gating system for optimizing the casting quality. Harmonic response analysis is performed to derive the vibration response incurred by the pneumatic hammer and to predict the maximum principal stress on the notch. The fatigue damage at the notch is evaluated using the modified Goodman theory. The suitability of the proposed scheme is demonstrated via processing experiments and numerical simulations. The proposed method is quicker, safer, and cleaner than traditional grinding cutoff processes and is thus a promising cost-effective method for application in the investment casting industry.

**Keywords** Investment casting · Vibration · Mold flow analysis

P.-H. Huang (✉) · Y.-T. Chen · B.-T. Wang
Department of Mechanical Engineering, National Pingtung University of Science and Technology, Pingtung 912, Taiwan, Republic of China
e-mail: phh@mail.npust.edu.tw

## 1 Introduction

Investment casting, also known as lost-wax casting, is one of the oldest known metal-forming processes for producing net-shaped components. This process produces casting components with accuracy, repeatability, versatility, and integrity from a variety of metals and functional alloys [1–4]. In the final stage of investment casting, the ceramic shell mold is removed and the ingates of gating system are cutoff for separating the parts from the casting tree. Conventionally, cutting the ingates is performed by sawing using grinding wheels, which consumes a great deal of labor, material cost, and processing time. The present study thus uses frequency response analyses to develop a fatigue damage method for separating casting parts from the casting tree to replace the sawing operation of traditional cutting machines.

Vibration dynamics are extensively utilized in various devices, such as the defroster in freezers, rock drillers, vibration cushions, quarrying machines, and vibration screening machines. The vibratory characteristics of an investment casting tree are applied here to efficiently cutoff ingates. Abdul-Karem et al. [5] applied vibration to thin wall castings to investigate liquid metal filling in thin section regions. Parloo et al. [6] applied a suspended, elastic structure with a free boundary to simulate the sensitivity of vibration modal parameters. Mohanty and Rixen [7] proposed theoretical equations of the vibration mode under harmonic excitation. They used the exciter to produce excitation and obtained the harmonic excitation frequency using an accelerometer. Wang et al. [8] conducted a finite element analysis (FEA) and modal response experiments using various boundary conditions to obtain the structural vibration characteristics.

Metallic mold flow analyses have been conducted to understand the filling and solidification of mold cavities during casting and to predict potential defects. Hwang and Stoehr [9–12] applied the marker and cell (MAC) and simplified

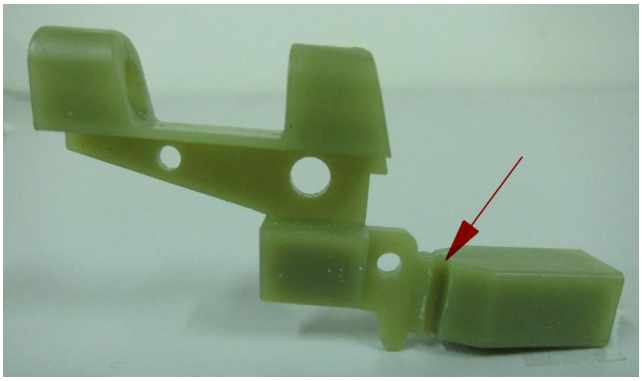

**Fig. 1** Configuration of wax pattern of the socket component. The *red arrow* shows the V-shaped notch near the ingate

MAC (SMAC) methods in a numerical simulation of the casting process using computational fluid dynamics (CFD) based on the finite difference method (FDM). Hirt [13] used the solution algorithm-volume of fluid (SOLA-VOF) method to analyze casting processes. The SOLA-VOF method allows the surface tension and wall adhesion to be evaluated from the orientation of the free surface. Anzai and Niyama [14] developed quasi-three-dimensional (3D) SMAC, which uses component thickness to simplify the 3D fluid field problem into a two-dimensional computation. Nomura et al. [15] extended the SMAC computation method into a full 3D computation model. Minaie et al. [16] used the semi-implicit method for pressure-linked equations (SIMPLE) method to analyze casting filling and condensation during the casting process. Hartmann et al. [17] applied computer-aided engineering (CAE) software in a simulation and found that the design of the casting spout directly affects the casting quality and that a poor design may result in component defects. Joseph et al. [18] designed two runners through experiments and CAE simulations, and compared the finished products with their simulation results. Chattopadhyay [19] estimated the solidification time of simple-shaped molds using finite volume-based numerical computation. Thammachot et al. [20] developed an optimal gating system design for the investment casting of sterling silver using computer-assisted simulation. Wang et al. [21, 22] adopted the FDM to model the low-pressure die casting of a magnesium wheel and the billet continuous processes. O'Mahoney and Browne [23] used experiments and an inverse method to study interface heat transfer during solidification. Homayonifar [24] investigated splashing and air entrapment in high-pressure die casting using a mixed VOF-Lagrange algorithm. In the present study, ProCAST software [13, 25–28], based on the SOLA-VOF algorithm, is used to determine the fluid thermodynamics and the finite element method is used for grid construction. Using mold filling analysis, the layout of the gating system and the pattern tree were designed to ensure good quality of the casting components.

## 2 Numerical analyses and experimental methods

In order to guarantee that the vibration-induced damage occurred close to the ingate without affecting the component structure, the size and geometry of the ingate were designed to generate a stress concentration for vibration cutoff. A V-shaped notch was made at the ingate section to produce the effect of stress concentration during vibration. Since the V-shaped notch reduced the cross-sectional area of the gating system, resulting in a transient turbulence of the molten metal streams near the changes of sections, mold filling analysis based on ProCAST software was conducted for simulating the pouring and casting processes to predict shrinkage, porosity, and casting deficiencies. The case considered in this study is the 24-cavity investment casting of steel sockets for a staple gun, as shown in Fig. 1. The casting material used was commercial medium carbon steel (JIS S35C). The sockets were cast in a controllable casting machine. The shell mold was made of a ceramic shell (zirconium sand) with a thickness of 10 mm. The shell mold was preheated to 1,250 °C, at which point the melted carbon steel with a temperature of 1,600 °C was poured into the mold. The casting parameters are summarized in Table 1.

This study used ANSYS software to analyze and obtain the theoretical modal parameters of casting trees for cases with fixed and free boundaries. Figures 2a, b show the finite element models of a casting tree used to obtain the vibration characteristics of the casting tree for free and fixed boundaries, respectively. The corresponding simulation parameters are summarized in Table 2. The settings used for constructing the finite element model are:

1. Element type: Linear 3D elements (solid 45).
2. Division type: Mapped mesh, number of elements is 113680, and number of nodes is 28560.
3. Boundary settings:

**Table 1** Summary of casting parameters

| Casting material | Shell material | $h_{shell\ mold}$ | $T_{shell\ mold}$ | $T_{pouring}$ | $T_{ambient}$ | $t_{sintering}$ |
|---|---|---|---|---|---|---|
| S35C | Zr sand | 10 mm | 1,250 °C | 1,600 °C | 40 °C | 30 min |

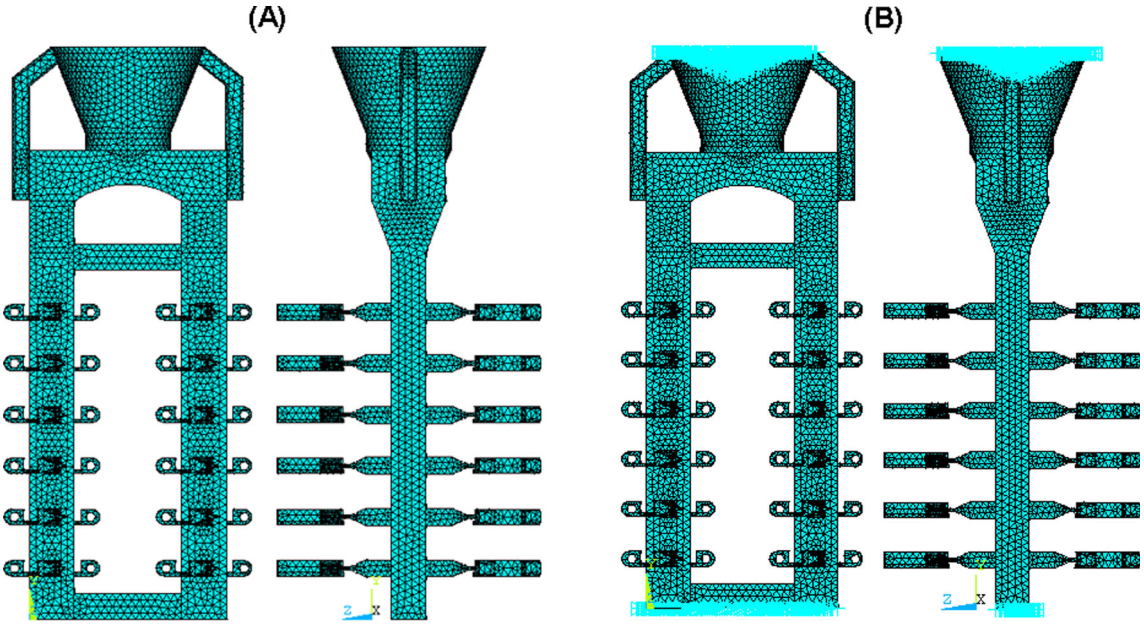


**Fig. 2** Configuration of FEA meshes for ANSYS analyses. **a** Free and **b** fixed boundary conditions

a. Free boundaries: No displacement constraint.
b. Fixed boundaries: The top and bottom of the pattern tree are fixed at UX=UY=UZ=0.

4. External load:

a. Free boundaries: Not available in modal analysis.
b. Fixed boundaries: *Y*-direction forces were exerted on the top and bottom of the pattern tree for the harmonic response analyses.

Through experimental modal analysis, this study obtained the structural vibration characteristics of the casting tree for the free boundary condition (as shown in Fig. 3) and the fixed boundary condition (as shown in Fig. 4). There were a total of 24 setting points, including two horizontally symmetric positions and six vertically symmetric positions. With an impact hammer as the driver and an accelerometer attached to the casting tree as the sensor, this study used the impact hammer to knock the casting tree to generate a vibration response in the structure, and then measured the vibration response using the accelerometer. Moreover, graphical analysis software was used to obtain the natural frequency, vibration mode, damping ratio, and frequency response function of the casting tree.

## 3 Results and discussion

A vertical gating system was adopted in this study. It comprised of a pouring basin, a sprue, a well, and a runner. Each socket mold cavity was connected to the runner via a V-shaped notch ingate. Since the V-shaped notch reduces the cross-sectional area of the gating system, it would increase the transient turbulence, splashing, and discontinuity of the molten metal streams near the changes of sections. Such unstable flows change the mold filling properties, such as density, viscosity, surface tension, and the onset of solidification, and further lead to the formation of casting defects after cooling, such as shrinkage, gaseous entrapment, and incomplete filling. To avoid defects during casting, mold flow analysis was conducted before the pouring processes started. The numerical simulation of mold filling was based on three constitutive equations for mass, momentum, and energy conservations, respectively. These equations, expressed in differential form,

**Table 2** Summary of material parameters of S35C for FEA and mold filling analysis

| Density ($\rho$) | Volume ($V$) | Poisson ratio ($\upsilon$) | Latent heat |
|---|---|---|---|
| 7,870 kg/m$^3$ | $7.5862\times10^{-4}$ m$^3$ | 0.29 | 207.15 kJ/kg |
| Thermal conductivity ($k$) | Dynamic viscosity ($\mu$) | Solidus temperature ($T_s$) | Surface tension ($\gamma$) |
| 50.80 W/m·K | 0.0033841 kg/m·s | 1,463.88 °C | 1.7028 N/m |
| Liquidus temperature ($T_l$) | $S_y$ | $S_{ut}$ | $S_e$ |
| 1,501.13 °C | 314 MPa | 569 MPa | 225 MPa |

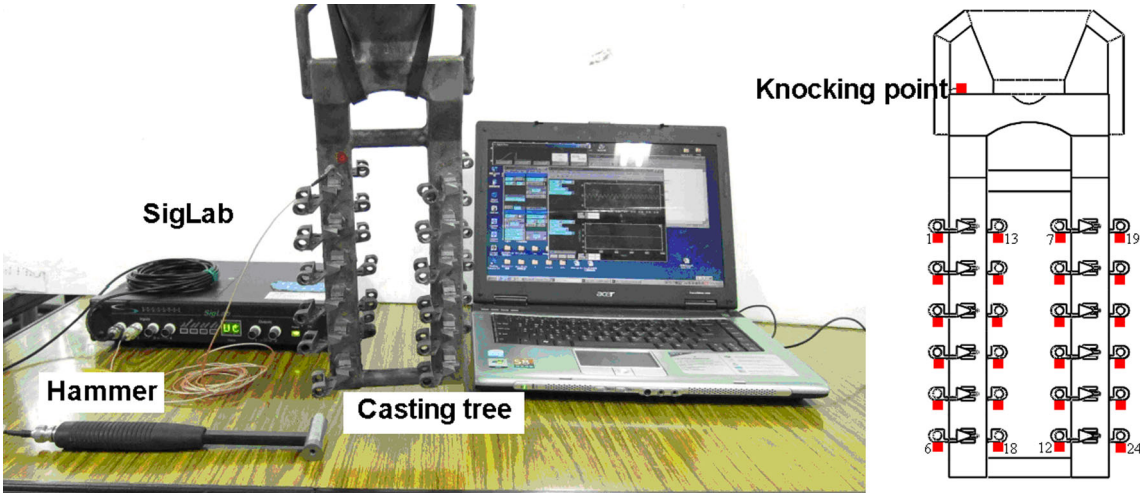


**Fig. 3** Experiments of frequency response for case with free boundary. *Red points* indicate the knocking point and the measured points

are referred to as Navier–Stokes equations and are given as follows [25]:

$$\frac{\partial \rho}{\partial t} + \nabla\cdot(\rho v) = 0 \tag{1}$$

$$\rho\left(\frac{\partial v}{\partial t} + v\cdot\nabla v\right) = -\nabla p + \mu\nabla^2 v + f_b \tag{2}$$

$$\rho\, C_v\left(\frac{\partial T}{\partial t} + v\cdot\nabla T\right) = -\nabla q - T\left(\frac{\partial p}{\partial T}\right)_{\rho}(\nabla v) \tag{3}$$

where $v$, $\rho$, $f_b$, and $\nabla p$ represent the velocity vector, density, body forces, and pressure gradient, respectively. $T$ is the temperature, $C_v$ is the specific heat, $q$ is the heat flux, and $t$ is time. The $\mu\nabla^2 v$ term denotes the quantity of shear stress ($\nabla^2$ is the vector Laplacian) when the fluid is assumed to be incompressible, homogeneous, and Newtonian ($\mu$ is the dynamic viscosity). The transient, laminar Navier–Stokes equations for a Newtonian fluid form the basis of the thermodynamics model. In a simulation of filling flow coupled with thermal transfer, the molten metal flow phenomena are governed by Eqs. (1)–(3). The 3D finite element method incorporated VOF formulations was adopted to track the motions of the free surface and metallic liquid flow. The asymmetric iterative scheme with accuracy on the order of $10^{-4}$ was adopted for convergence, which permits an accurate simulation of the filling transient of the metal castings and the subsequent convection and contraction [25]. Figure 5 shows the temperature evolution of the pouring system. The pouring process was completed at about ~8 s. As shown, the temperature of the casting began to decrease after the pouring process had finished. When the filling was complete, the temperature at the bottom of the investment casting component was 1,500 °C. About tens of seconds later, the bottom of the casting tree began to solidify, coming very close to the

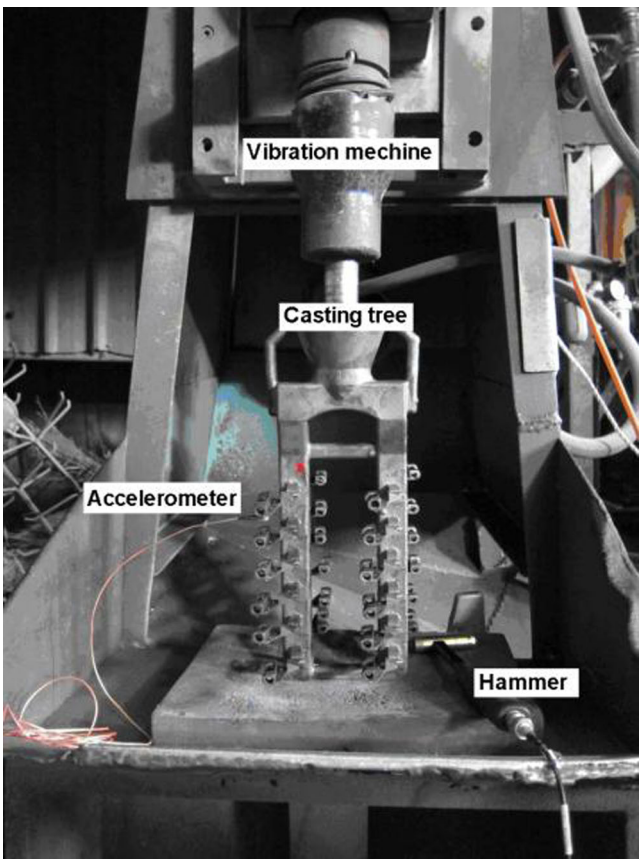


**Fig. 4** Experiments of frequency response for case with fixed boundary

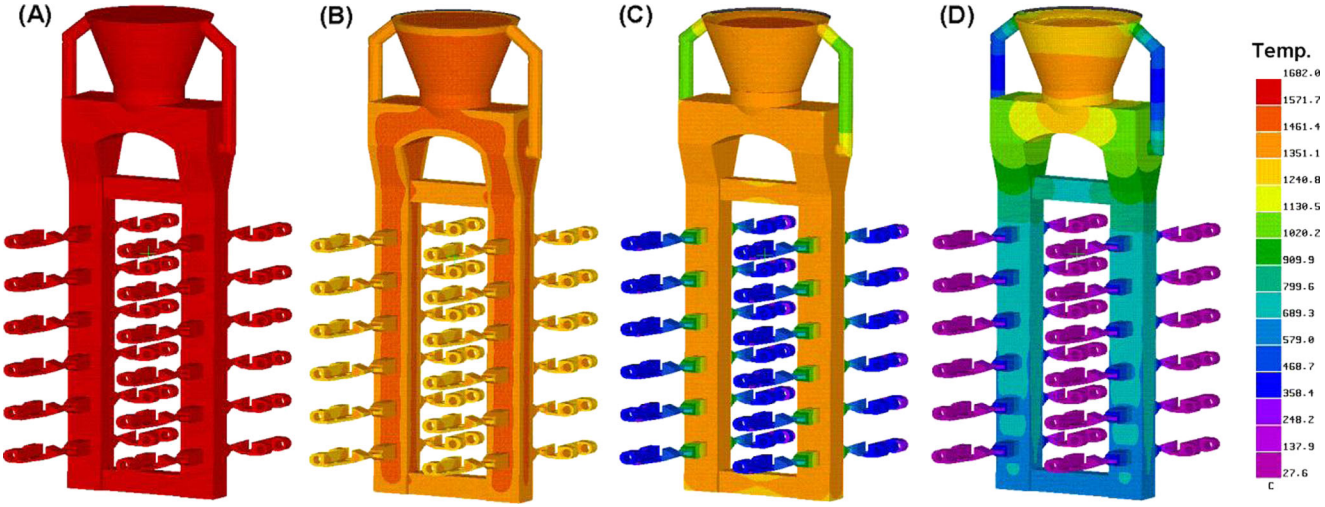


**Fig. 5** Temperature evolution of pouring system at $t$=**a** 15, **b** 420, **c** 8,100, and **d** 30,000 s

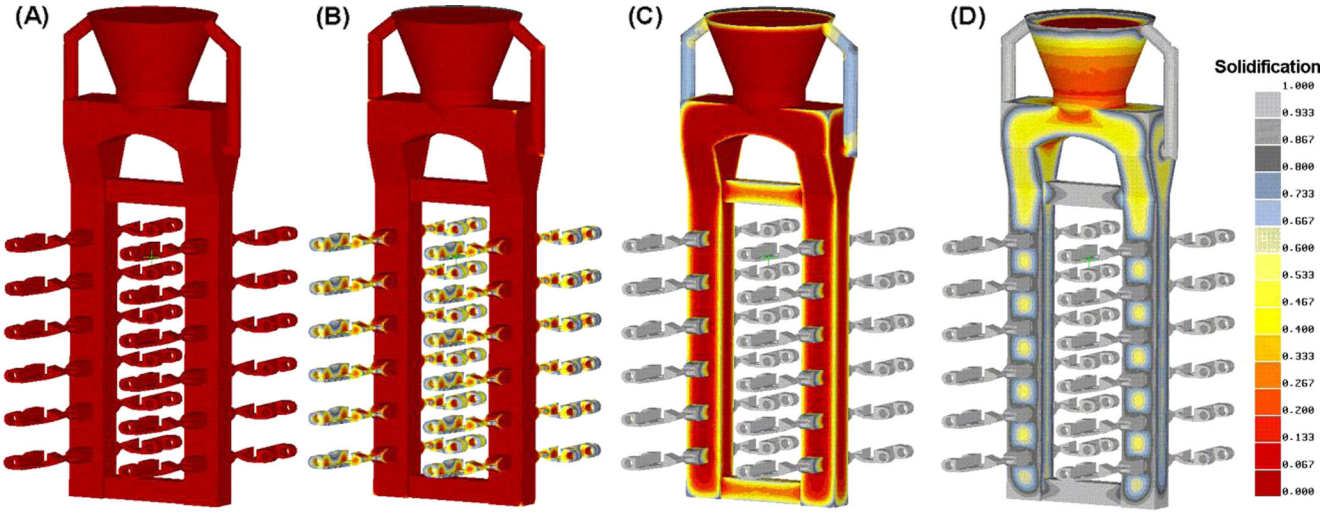


**Fig. 6** Solidification evolution of pouring system at $t$=**a** 15, **b** 600, **c** 2,800, and **d** 7,200 s

coagulation temperature (~1,463 °C). At a time of 30,000 s, the temperature of the casting components decreased to 150 °C.

Figure 6 shows the simulation results of solidification evolution of the modified pouring system. The results of mold filling analysis showed that the molten metallic

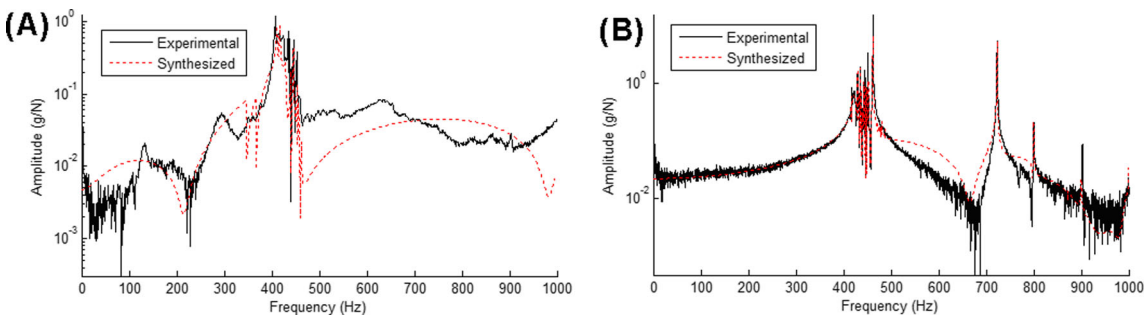


**Fig. 7** Frequency responses of casting tree for **a** fixed and **b** free boundary conditions

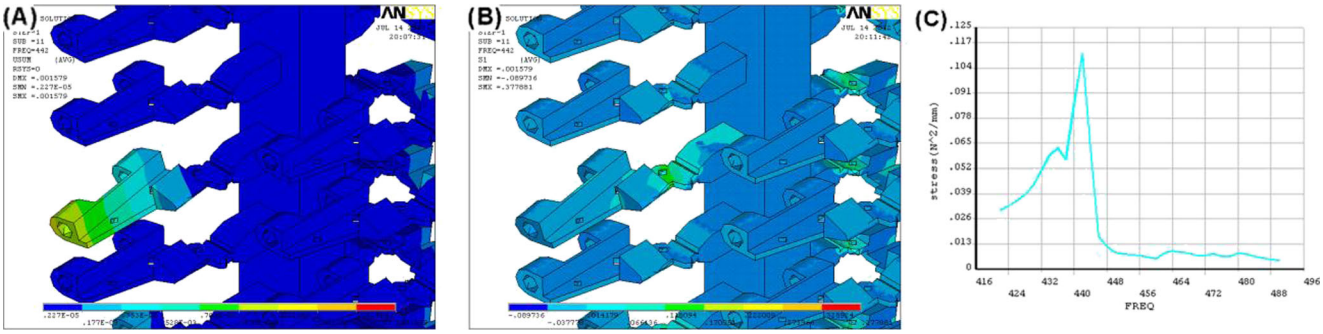


**Fig. 8** Harmonic response analyses for casting tree. **a** Displacement, **b** maximum principal stress, and **c** relation between frequency and stress

liquids could flow into and fill up each cave of the casting pattern tree after 10 s. The time required from pouring to full coagulation of the component was approximately 2 h. After the casting had cooled, no shrinkage, gaseous entrapment, or incomplete filling was observed, suggesting that the modified casting scheme was feasible. The V-shaped notches based on the results of mold flow analysis were designed to be 1.5 mm in depth at a distance of 2 mm from the inlet. As shown in Fig. 1, the V-shaped notches were made at the inlet section of the wax pattern before the pouring was processed.

Figure 7a, b shows the frequency response function of the casting tree for the fixed and free boundaries, respectively. The black solid line was obtained from the experiment and the red dotted line represents the results of synthesized analyses. The structural modal parameters derived from the embedded curves were the natural frequency, vibration modal type, and modal damping ratio. As shown, the natural frequency of the casting tree was between 400 and 460 Hz. The harmonic response of the casting tree was further analyzed. The analyses showed that the vibration mode was vertically upward and downward at a frequency of 443 Hz, which meets the requirement of vibration cutoff at the ingate of the runner. Moreover, using the results of harmonic response analyses, the corresponding parameters of displacement, and maximum principal stress and the frequency vs. stress relations were obtained, as shown in Fig. 8.

Figure 8a shows the displacement change distribution. The generated modal shapes during vibration indicate that the displacement swing of the casting tree was located only at the V-shaped notches. Moreover, the maximum and minimum principal stresses (597.1 and −161.7 MPa, respectively) were generated around the V-shaped notches at a frequency of 446 Hz, as shown in Fig. 8b, c. The results of ANSYS analyses agree very well with the experimental frequency responses. The corresponding mean stress ($S_m$) and alternating stress ($S_a$) were calculated to be 217.7 and 379.4 MPa, respectively.

In materials science and mechanical design fields, the Goodman, Soderberg, Gerber, and modified Goodman theories are commonly used to quantify the effect of the interaction of mean and alternating stresses on the fatigue life of a material [29–31]. The present work uses the modified Goodman criterion to predict whether the V-shaped notches of the ingate may be damaged during vibration. The material properties necessary to construct the modified Goodman diagram are yield strength ($S_y$), ultimate strength ($S_{ut}$), and fatigue strength ($S_e$) for a given life. These mechanical properties for S35C have slightly different values in experimental reports [32–34]. Here, the values of $S_y$=314, $S_{ut}$=569, and $S_e$= 225 MPa [32] were adopted in the analysis. As shown in Fig. 9, the modified Goodman diagram can be plotted from the intersection of (i) the line connecting the material ultimate and fatigue strengths with (ii) a 45° sloped line, originating from the monotonic yield strength of the material. The criterion equation of the line CD for the modified Goodman relation is given by:

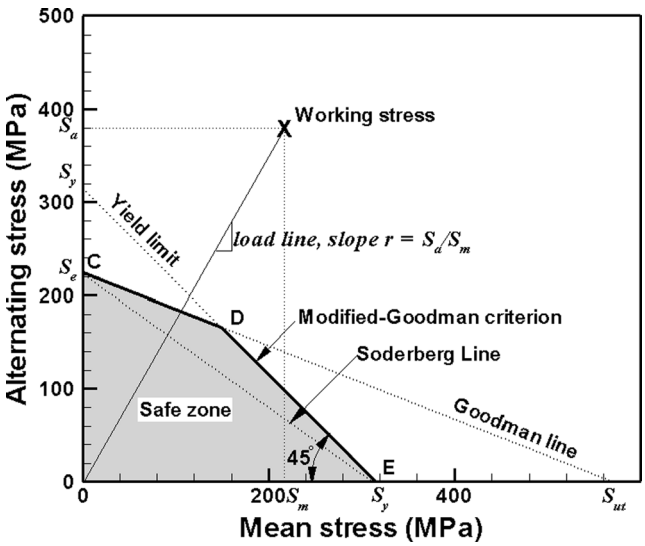


**Fig. 9** Predictions and analyses of fatigue damage based on the modified Goodman criterion

$$\frac{S_a}{S_e} + \frac{S_m}{S_{ut}} = 1 \tag{4}$$

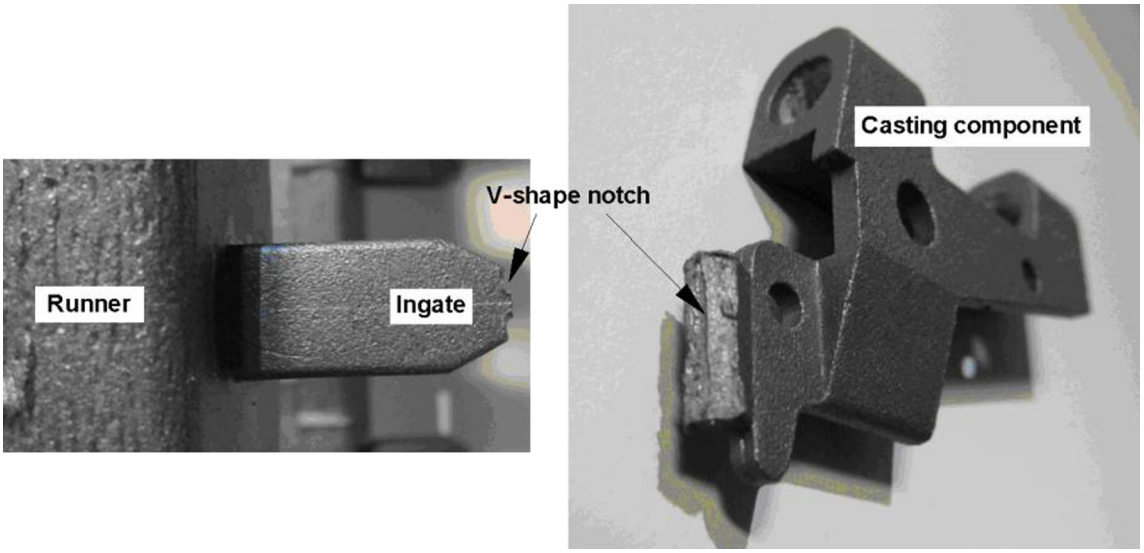


**Fig. 10** Configurations of the cutoff position (*left*) and the disjointed casting component

Similarly, the modified Goodman relation for line segment DE (i.e., the yield limit) is:

$$S_a + S_m = S_y \tag{5}$$

where $S_a$ is the alternating stress and $S_m$ is the mean stress. The general tendency given by the modified Goodman relation is one of decreasing fatigue life with increasing mean stress for a given level of alternating stress, as shown in Fig. 9. The relation can be constructed to determine the safe cyclic loading of a component; if the coordinate given by the mean stress and the alternating stress lies under the curve given by the relation, then the component will be safe (i.e., the gray zone of Fig. 9). If the coordinate is above the curve, then the component will fail for the given stress parameters. According to the analysis results (Fig. 8), the stress values at the V-shaped notch induced by the dynamic vibration are $S_m$=217.7 MPa and $S_a$= 379.4 MPa. It is observed that the working stress is outside the safe zone (Fig. 9), and thus it can be predicted that the investment casting components could be separated by the vibration.

To verify the suitability of the proposed scheme, a casting tree was clamped to a vibration machine for a vibrating cutoff experiment. The vibration machine was driven by a pneumatic cylinder. The impact frequency of the vibration machine was around 450 Hz. Since the vibrations exerted a bending stress on the ingate, the effect of stress concentration led to the ingate region sustaining a continuous tensile/compressive stress. After about 15 s, the ingates of the casting components exhibited fatigue damage, and the casting components became disjointed from the casting tree. The duration of the vibration separation process was about 25 s (i.e., all casting components were completely separated from the casting tree). One of the separated casting components is shown in Fig. 10. It can be observed that the disjunction is located only at the position of the V-shaped notch.

In the proposed scheme, the vibration-induced fatigue damage by a pneumatic hammer machine is used to separate casting parts from the casting tree to replace traditional sawing using a grinding wheel cutting machine. The pneumatic hammer machine and the CAE software are commonly used in commercial foundries, and thus the proposed method requires no extra expenditure in terms of equipment cost. The proposed scheme reduces the use of grinding wheels and requires only one eighth of the traditional processing time and labor costs. Excluding the pre-design cost, the proposed scheme can save $6,500 per year for the studied case with an annual production of 100,000 pieces. The cost savings increase with increasing the quantity of products. In addition, the proposed solution is safe, energy saving, and environmentally-friendly.

## 4 Summary

Frequency response analyses were conducted to develop a fatigue damage method for disjointing the casting components to replace the cutting operation of traditional cutting machines. A V-shaped notch was made at the inlet section to produce the effect of stress concentration during vibration. Pouring experiments were conducted to verify the accuracy of mold flow analysis. Experimental results showed that the proposed scheme is much better than the traditional grinding cutoff method in terms of processing time, operation efficiency, and labor and material costs.

**Acknowledgments** The authors acknowledge the National Science Council of Taiwan for financially supporting this research under grant

NSC 102-2221-E-020-020. The authors are also grateful to MIRDC, Taiwan, for supporting ProCAST software.

## References


1. Pattnaik S, Karunakar DB, Jha PK (2012) Developments in investment casting process—a review. J Mater Proc Technol 212:2332–2348
2. Jones S, Yuan C (2003) Advances in shell moulding for investment casting. J Mater Proc Technol 135:258–265
3. Sabau AS, Viswanathan S (2003) Material properties for predicting wax pattern dimensions in investment casting. Mater Sci Eng A-Struct 362:125–134
4. Niyama E, Anzai K (1995) Solidification velocity and temperature gradient in infinitely thick alloy castings. Mater Trans 36(1):61–64
5. Abdul-Karem W, Green N, Al-Raheem KF (2012) Vibration-assisted filling capability in thin wall investment casting. Int J Adv Manuf Technol 61:873–887
6. Parloo E, Verboven P, Guillaume P, Overmeire M (2003) Force identification by means of in-operation modal model. J Sound Vib 262:161–173
7. Mohanty P, Rixen D (2004) Operational modal analysis in the presence of harmonic excitation. J Sound Vib 270:93–109
8. Wang BT, Lin CH, Lee KT (2003) Experimental modal analysis and model verification of vibrator coil structure. 20th National Conference on Mechanical Engineering of CSME, pp 529–536
9. Hwang WS, Stoehr RA (1988) Molten metal flow pattern prediction for the complete solidification analysis of near net shape casting. Mater Sci Technol-Lond 4:240–250
10. Hwang WS, Stoehr RA (1983) Fluid flow modeling for computer-aided design of castings. Int J Miner Metall Mater 35(10):22–29
11. Hwang WS, Stoehr RA (1988) Modeling of fluid flow. ASM Metals Handbook, 9th edn. 15:11(B):867–876
12. Hwang WS, Stoehr RA (1987) Computer simulation for the filling of castings. Trans AFS 97:425–430
13. Hirt CW (1983) Flow analysis for non-expects. PCMCW II, pp 67–75
14. Anzai K, Niyama E (1988) Quasi three-dimensional mold filling simulation system for prediction of defects in die castings. Conference proceeding on the modeling of casting, welding and advanced solidification processes IV, pp 471–485
15. Nomura H, Terashima K, Keishima K (1991) Prediction of die casting flow behavior by three dimensional simulation. Imono 63: 425–430
16. Minaie B, Stelson KA, Voller VR (1991) Analysis of flow patterns and solidification phenomena in the die casting process. J Eng Mater Technol (Trans ASME) 113(3):296–302
17. Hartman C, Kokot V, Seefeldt R (2003) Numerical optimization of casting processes-leveraging coupled process and multi-object optimization to the manufacturing level. International congress on FEM technology, pp 12–14
18. Joseph H, Clerry P, Alguine V, Nguyen T (1999) Simulation on die filling in gravity die casting using SPH and MAGMASOFT. CRC for alloy and solidification technology (CAST), pp 423–428
19. Chattopadhyay H (2011) Estimation of solidification time in investment casting process. Int J Adv Manuf Technol 55:35–38
20. Thammachot N, Dulyapraphant P, Bohez ELJ (2013) Optimal gating system design for investment casting of sterling silver by computer-assisted simulation. Int J Adv Manuf Technol 67:797–810
21. Wang YC, Li DY, Peng YH, Zeng XQ (2007) Numerical simulation of low pressure die casting of magnesium wheel. Int J Adv Manuf Technol 32:257–264
22. Wang YC, Li DY, Peng YH, Zhu LG (2007) Computational modeling and control system of continuous. Int J Adv Manuf Technol 33:1–6
23. O'Mahoney O, Browne DJ (2000) Use of experiment and an inverse method to study interface heat transfer during solidification in the investment casting process. Exp Thermal Fluid Sci 22:111–122
24. Homayonifar P, Babaei R, Attar E, Shahinfar S, Davami P (2008) Numerical modeling of splashing and air entrapment in high-pressure die casting. Int J Adv Manuf Technol 39:219–228
25. Website, http://www.esi-group.com/products/casting/procast, 2011
26. Bellet M, Decultieux F, Menai M, Bay F, Levaillant C, Chenot JL, Schmidt P, Svensson IL (1996) Thermomechanics of the cooling stage in casting processes: three-dimensional finite element analysis and experimental validation. Metall Mater Trans B 29(B):81–99
27. Drezet JM, Rappaz M (1996) Modeling of ingot distortion during direct chill casting of aluminum alloys. Metall Mater Trans A 27(A): 3214–3225
28. Sabau AS (2006) Alloy shrinkage factors for the investment casting process. Metall Mater Trans B 37(1):131–140
29. Goodman J (1899) Mechanics applied to engineering. Longman, Green & Company, London
30. Hertzberg RW (1996) Deformation and fracture mechanics and engineering materials. Wiley, Hoboken
31. Mars WV (2009) Computed dependence of rubber's fatigue behavior on strain crystallization. Rubber Chem Technol 82(1):51–61
32. Miao DH, Nishida SI, Hattori N (2008) Effect of pre-strain of fatigue properties of carbon steel. Eng Mech 25(12):147–152
33. Endo M, McEvily AJ, Matsunaga H, Eifler D (2006) The growth of short cracks from defects under multi-axial loading. Fracture of nano and engineering materials and structures, pp 1219–1220
34. McEvily AJ, Endo M, Ishihara S (2005) The influence of biaxial stress on the fatigue behaviour of defect-containing steels. ICF11